

Available at www.sciencedirect.comjournal homepage: www.elsevier.com/locate/watres

Virus disinfection in water by biogenic silver immobilized in polyvinylidene fluoride membranes

Bart De Gusseme^a, Tom Hennebel^a, Eline Christiaens^a, Hans Saveyn^b, Kim Verbeke^c, Jeffrey P. Fitts^d, Nico Boon^a, Willy Verstraete^{a,*}

^a Department of Biochemical and Microbiological Technology, Laboratory of Microbial Ecology and Technology (LabMET), Ghent University, Coupure Links 653, B-9000 Gent, Belgium

^b Department of Applied Analytical and Physical Chemistry, Particle and Interfacial Technology Group (PaInt), Ghent University, Coupure Links 653, B-9000 Gent, Belgium

^c Department of Metallurgy and Materials Science, Ghent University, Technology Park 903, B-9052 Gent, Belgium

^d Environmental Sciences Department, Brookhaven National Laboratory, Building 830, Upton, NY 11973, USA

ARTICLE INFO

Article history:

Received 1 September 2010

Received in revised form

26 November 2010

Accepted 29 November 2010

Available online 7 December 2010

Keywords:

Antimicrobial

Ionic silver

Metallic silver

X-ray absorption spectroscopy (XAS)

ABSTRACT

The development of innovative water disinfection strategies is of utmost importance to prevent outbreaks of waterborne diseases related to poor treatment of (drinking) water. Recently, the association of silver nanoparticles with the bacterial cell surface of *Lactobacillus fermentum* (referred to as biogenic silver or bio-Ag⁰) has been reported to exhibit antiviral properties. The microscale bacterial carrier matrix serves as a scaffold for Ag⁰ particles, preventing aggregation during encapsulation. In this study, bio-Ag⁰ was immobilized in different microporous PVDF membranes using two different pre-treatments of bio-Ag⁰ and the immersion-precipitation method. Inactivation of UZ1 bacteriophages using these membranes was successfully demonstrated and was most probably related to the slow release of Ag⁺ from the membranes. At least a 3.4 log decrease of viruses was achieved by application of a membrane containing 2500 mg bio-Ag^{0 powder} m⁻² in a submerged plate membrane reactor operated at a flux of 3.1 L m⁻² h⁻¹. Upon startup, the silver concentration in the effluent initially increased to 271 µg L⁻¹ but after filtration of 31 L m⁻², the concentration approached the drinking water limit (= 100 µg L⁻¹). A virus decline of more than 3 log was achieved at a membrane flux of 75 L m⁻² h⁻¹, showing the potential of this membrane technology for water disinfection on small scale.

© 2010 Elsevier Ltd. All rights reserved.

1. Introduction

Contamination of drinking water and the subsequent outbreak of waterborne diseases are the leading cause of death in many developing nations. Therefore, virus removal during water treatment has received more attention due to the epidemiological significance of these pathogens (Rose and Gerba, 1991). Especially for drinking water purposes, the

development of innovative water disinfection strategies is of utmost importance. Recently, enteric viruses were included in the US EPA's new Contaminant Candidate List and thus they may become subject to the drinking water quality standards (USEPA, 2009).

Significant interest has arisen in the use of silver containing nanoparticles for water disinfection (Li et al., 2008). Several authors have reported on the antiviral activity of

* Corresponding author. Tel.: +32 9 264 59 76; fax: +32 9 264 62 48.

E-mail address: Willy.Verstraete@UGent.be (W. Verstraete).

URL: <http://www.labmet.ugent.be>

0043-1354/\$ – see front matter © 2010 Elsevier Ltd. All rights reserved.

doi:10.1016/j.watres.2010.11.046

silver nanoparticles (nAg^0), for example against HIV-1 (Elichiguerra et al., 2005; Rogers et al., 2008). Recently, inactivation of bacteriophages and murine noroviruses was also demonstrated in disinfection assays using biogenic silver ($bio-Ag^0$) (De Gussemme et al., 2010b). The latter material consists of silver particles of 11.2 ± 0.9 nm, produced by reduction of ionic silver on the bacterial cell surface of *Lactobacillus fermentum* (Sintubin et al., 2009). The attachment of the silver particles to a bacterial carrier matrix of micrometer scale prevents them from aggregating, which is an advantage over chemically produced nAg^0 particles which tend to aggregate in aqueous solutions at high concentrations or when their average particle size is lower than 40 nm (Mafune et al., 2000). Moreover, the bacterial surface serves as a scaffold that facilitates the incorporation of biogenic metals into a supporting material, thus preventing the nanoparticles from leaching into the environment. This has been demonstrated for biogenic palladium nanoparticles (Hennebel et al., 2010, 2009a, 2009b), but not yet for biogenic silver nanoparticles.

In the past decade, membrane based technologies have been increasingly applied to improve the water quality. Although viruses are smaller than the pore sizes used in microfiltration processes, they are retained by biofilms that foul the membranes (Ueda and Horan, 2000; Wu et al., 2010). The formation of these biofilms is unwanted because of the related decrease in membrane flux, increasing energy costs and shorter membrane life (McDonogh et al., 1994). To cope with this problem, silver can be applied for both biofouling and virus control, by coating nAg^0 directly on the surface of the membranes or by embedment in the polymer matrix of the membrane itself (Yang et al., 2009; Zodrow et al., 2009). Zodrow et al. (2009) have prepared nAg^0 incorporating membranes by means of the 'phase inversion' technique, during which the polymer is transformed from a liquid to a solid phase in a controlled manner (Mulder, 1991; Vankelecom, 2002). More specifically, the 'immersion-precipitation' method was applied, in which the solvent solution containing the polymer and nAg^0 (i.e. the casting dope) was casted on a support and then immersed in a water (= non-solvent) bath to effect polymer precipitation (Vankelecom, 2002). Zodrow et al. (2009) have shown a significant improvement in the removal of bacteriophage MS2 by incorporating nAg^0 . Moreover, the addition of silver prevented bacterial attachment and biofilm formation. The authors suggested the release of Ag^+ to be the main mechanism for both outcomes.

The aim of this study was to incorporate silver in polymeric membranes in order to develop a disinfecting material based on immobilized biogenic silver nanoparticles. Therefore, the immersion-precipitation technique was used to prepare the membranes, and the structure and the antiviral properties of this material were examined. The goal of this research was preparing a casting dope without addition of a dispersing agent. Two pre-treatments of the biogenic silver were therefore investigated: centrifugation of a $bio-Ag^0$ suspension (' $bio-Ag^0_{susp}$ ') and spray-drying to a powder (' $bio-Ag^0_{powder}$ '). Batch and continuous disinfection assays with the different membranes were conducted in water contaminated with the bacteriophage UZ1, a model for enteric viruses (Verthé et al., 2004).

2. Materials and methods

2.1. Production of biogenic silver

$Bio-Ag^0$ was produced with *L. fermentum* LMG 8900 (LMG culture collection, Ghent University, Belgium) according to Sintubin et al. (2009). Briefly, after *L. fermentum* biomass was harvested by subsequent centrifugation and washing in deionized water, the pH was increased with NaOH to 11.5, followed by the addition of a diamine silver complex in a ratio of 1:4.6 $Ag:CDW$ (cell dry weight). After 24 h, the produced biogenic silver was harvested by centrifugation and resuspended in deionized water. The resulting $bio-Ag^0$ suspension in water contained 15.890 g $Ag L^{-1}$ as determined by atomic absorption spectroscopy (AAS) after digestion (see below), and is referred to as ' $bio-Ag^0_{susp}$ '. The nanoparticles had a particle size of 11.2 ± 10.9 nm (Sintubin et al., 2009).

This suspension was fed into a Production Minor spray-dryer (Gea Niro, Soeberg, Denmark) with main spray chamber of 2700 mm \times 1400 mm. The feed flow rate used was 185 cm³ min⁻¹, and the inlet and outlet air temperatures were 200 °C and 95 °C. The atomization head was operated at $15,272$ rpm. A dry powder (' $bio-Ag^0_{powder}$ ') was obtained, containing 140 mg $Ag g^{-1}$ as determined by AAS after digestion (see below).

2.2. Membrane fabrication

Both $bio-Ag^0_{susp}$ and $bio-Ag^0_{powder}$ (defined in section 2.1) were used to produce polyvinylidene fluoride (PVDF) membranes. In the case of $bio-Ag^0_{susp}$, the suspension was centrifuged in 50 mL test tubes ($10,000\times g$ for 15 min) and the supernatant was removed. The remaining solids in the tubes (i.e. the wet pellet) were dispersed in *N,N*-dimethylformamide (DMF). In the case of $bio-Ag^0_{powder}$, the powder was directly added to DMF. Eventually, two DMF solutions were obtained for each of the two $bio-Ag^0$ formulations, containing 1000 and 10,000 mg $Ag L^{-1}$. The $bio-Ag^0$ particles were dispersed at 50 °C in an Elmasonic S30H ultrasonic bath (Elma, Singen, Germany) for 10 min. To each of the four dispersions 14 wt.% PVDF (Kynar 500®, Arkema, Amsterdam, The Netherlands) was slowly added under vigorous stirring at 50 °C. Finally, the dispersions were placed in an ultrasonic bath (50 °C, 10 min), in order to prepare homogeneous casting dopes. A similar casting dope without $bio-Ag^0$ was prepared as a control.

Membranes were fabricated using the direct immersion-precipitation method at 25 °C, as previously described (Hennebel et al., 2010). 30 mL of a casting dope was spread uniformly on a 0.12 m² non-woven support (Novatex FO 2471, Freudenberg, Germany) by means of an automatic film applicator (Elcometer 4340, Hermalle-sous-Argenteau, Belgium). The resulting wet film thickness was 250 μm (controlled by an Elcometer 3530 casting knife). DMF was allowed to evaporate for 30 s, and subsequently, the nascent film was immersed into a deionized water bath to allow polymer precipitation. The theoretical maximum silver content in the membranes made with the 1000 mg $Ag L^{-1}$ and $10,000$ mg $Ag L^{-1}$ casting dopes, was 250 mg $bio-Ag^0 m^{-2}$ and 2500 mg $bio-Ag^0 m^{-2}$, respectively.

2.3. Membrane characterization

Hydrophobicity of the membranes was determined by sessile drop contact angle measurements. After deposition of a water drop of 3 μL on the dry membrane surface, the contact angles were determined using the Krüss DSA10 drop shape analysis system (Sysmex, Hoeilaart, Belgium) and DSA Software 1.80. Values are the mean of 6 measurements per membrane surface. Membrane zeta potential was determined by measuring the streaming potential with a laboratory scale filter press according to Saveyn et al. (2005). A Fluke 189 Multimeter was connected to the cathode and anode side. All experiments were conducted in a 5 mM KNO_3 background solution at pH 7. Membrane morphology and bio- Ag^0 localization were studied on the top surfaces and cross sections of dried membranes, by means of scanning electron microscopy (SEM). The membrane cross sections were obtained by fracturing the membrane after immersion in liquid N_2 . The samples were sputter-coated with an ultrathin Au layer (Baltec AG, Balzers, Liechtenstein) and analyzed under vacuum with a FEI XL30 SEM (FEI, Eindhoven, The Netherlands) equipped with a LaB_6 filament and an energy dispersive X-ray spectroscope (EDAX, Tilburg, The Netherlands).

2.4. Growth and detection of bacteriophage UZ1

The stock of bacteriophage UZ1 was prepared as previously described (De Gussemé et al., 2010b). To detect phages, the soft agar layer method described by Adams (1959) was applied, using serial tenfold dilutions of the samples in SM medium (6.1 g L^{-1} Tris–HCl, 5.8 g L^{-1} NaCl, 1.2 g L^{-1} MgSO_4 , 0.1 g L^{-1} gelatin (Oxoid, Basingstoke, UK), pH 7.5) and a mid-log phase *Enterobacter aerogenes* BE1 culture LMG 22092 (LMG culture collection, Ghent University, Belgium) (De Gussemé et al., 2010a). Phages were counted as plaque forming units (pfu) and the phage concentration was expressed as pfu mL^{-1} . The limit of detection (LOD) was determined at 1.0×10^2 pfu mL^{-1} . When no viruses were detected in the samples, the LOD was used as a conservative estimate for the UZ1 concentration.

2.5. Virus inactivation in batch by bio- Ag^0 immobilized in PVDF membranes

All experiments were performed in bottled natural source water (Spa Blauw, Spadel, Brussels, Belgium) to which no free chlorine was added to avoid virus inactivation. The composition of the water was similar as previously reported (De Gussemé et al., 2010b). The batch experiments were conducted at 25 °C in sterilized 500 mL flasks on a magnetic stirrer. 25 cm^2 of the 250 mg bio- $\text{Ag}^0_{\text{susp}}$ m^{-2} , the 2500 mg bio- $\text{Ag}^0_{\text{susp}}$ m^{-2} , and the 2500 mg bio- $\text{Ag}^0_{\text{powder}}$ m^{-2} membranes were incubated in 200 mL water spiked with appr. 10^6 pfu mL^{-1} . Samples were taken at 0 h, 2 h and 24 h, and stored at 4 °C for further analysis. Silver in the samples for UZ1 detection was immediately quenched with an excess of thioglycolate-thiosulfate neutralizer (Tilton and Rosenberg, 1978).

2.6. Virus inactivation by bio- Ag^0 immobilized in PVDF membranes in a membrane reactor

The membrane sheets were fixed on both sides of a 0.06 m^2 plate cartridge with a spacer in between, rendering a total

membrane area of 0.12 m^2 . The plate membrane was submerged in a polycarbonate membrane reactor with a working volume of 8 L (Fig. S1). Before startup, the reactor vessel was filled with 8 L of the influent, natural source water spiked with phage UZ1 ($C_{\text{infl}} = 10^6$ pfu mL^{-1}). After installation of the membrane, the influent was further dosed at the bottom of the reactor and mixed by a pressurized air diffuser. The effluent pump was working semi-continuously, thus providing relaxation periods for the membrane. The airflow along the membrane and the relaxation periods facilitated the flux through the membrane (cross-flow principle). Reactor runs for each plate membrane were conducted at a flow rate and hydraulic retention time (HRT) of 0.375 L h^{-1} and 1 d, respectively. In a subsequent reactor run, an additional 2500 mg bio- $\text{Ag}^0_{\text{powder}}$ m^{-2} plate membrane of the same size was used at a flow rate of 8 L h^{-1} , resulting in a HRT of 1 h. Influent, bulk and effluent samples were taken at regular intervals and stored at 4 °C for further analysis. The filtrate sample at time 0 h was taken immediately after installation of the membranes. Silver in the samples for UZ1 detection was immediately quenched.

2.7. Silver measurements

The concentration of silver in the bio- $\text{Ag}^0_{\text{susp}}$ and bio- $\text{Ag}^0_{\text{powder}}$ stock solutions was measured by atomic absorption spectroscopy (AAS) (Shimadzu AA-6300, Japan), after digestion according to Sintubin et al. (2009). The LOD of AAS was 0.1 mg L^{-1} . The concentration of silver in the samples of the batch and reactor experiments were determined by means of ICP-MS (Elan DRC-e, Perkin Elmer, MA, USA). The LOD of ICP-MS was 0.8 $\mu\text{g L}^{-1}$.

3. Results

3.1. Characterization of the PVDF membranes

Both formulations of biogenic silver, bio- $\text{Ag}^0_{\text{susp}}$ and bio- $\text{Ag}^0_{\text{powder}}$, were immobilized in PVDF membranes using the direct immersion-precipitation method. Spray-drying of the bio- Ag^0 did not alter the chemical oxidation state of the metallic silver particles (see X-ray absorption spectroscopy analyses in Supplementary Data and Fig. S2). The membranes impregnated with bio- $\text{Ag}^0_{\text{powder}}$ had a similar contact angle and zeta potential as the membrane without bio- Ag^0 , regardless of bio- $\text{Ag}^0_{\text{powder}}$ concentration (Table 1). This contrasted with the bio- $\text{Ag}^0_{\text{susp}}$ membranes, which had an increased contact angle, thus making them more hydrophobic. In addition, there was a decline in the absolute value of the membrane zeta potential at both bio- $\text{Ag}^0_{\text{susp}}$ concentrations (Table 1). SEM images of the bio- $\text{Ag}^0_{\text{susp}}$ membrane in the backscattered electron (BSE) mode revealed the presence of silver containing structures, visible as enlightened dots at the rough and hydrophobic surface (Fig. 1A). By larger magnification, individual entities of nanoparticles could still be observed within these agglomerates. The presence of silver was confirmed by EDX (Fig. S3A) and the diameter of the agglomerates ranged from tens to hundreds of nanometers. Similar clusters were observed as bright structures throughout the cross section of the membrane in the BSE mode (Fig. 1B and Fig. S3B). The cross section revealed a uniform sponge-like structure, built by

Table 1 – Hydrophobicity of the different PVDF membranes expressed as contact angle ($n = 6$) and the membrane zeta potentials ($n = 3$). Values represent the means and their standard deviation.

Membrane	Contact angle (°)	Zeta potential (mV)
0 mg bio-Ag ⁰ m ⁻²	74.7 ± 4.0	-2.98 ± 0.80
250 mg bio-Ag ⁰ _{powder} m ⁻²	75.4 ± 6.9	-3.78 ± 0.48
2500 mg bio-Ag ⁰ _{powder} m ⁻²	73.7 ± 0.7	-2.97 ± 0.71
250 mg bio-Ag ⁰ _{susp} m ⁻²	123.6 ± 3.4	-0.60 ± 0.18
2500 mg bio-Ag ⁰ _{susp} m ⁻²	125.8 ± 1.8	-0.36 ± 0.06

densely packed polymeric crystallites with micropores in between. The thickness of the top layer of the bio-Ag⁰_{susp} membrane amounted to 35 μ m.

No silver agglomerates were observed in the BSE mode on the top surface of the membranes with bio-Ag⁰_{powder} (Fig. 1C). Although the presence of Ag on the hydrophilic surface was demonstrated by means of EDX (Fig. S3C), the amount was 3–5 times smaller compared to the membranes containing bio-Ag⁰_{susp}. The top surface was smoother and showed micropores with a diameter between 60.9 and 338.0 nm. In the 95 μ m thick cross section, the formation of a dense skin layer and a cellular sublayer was observed (Fig. 1D). The asymmetry of this type of

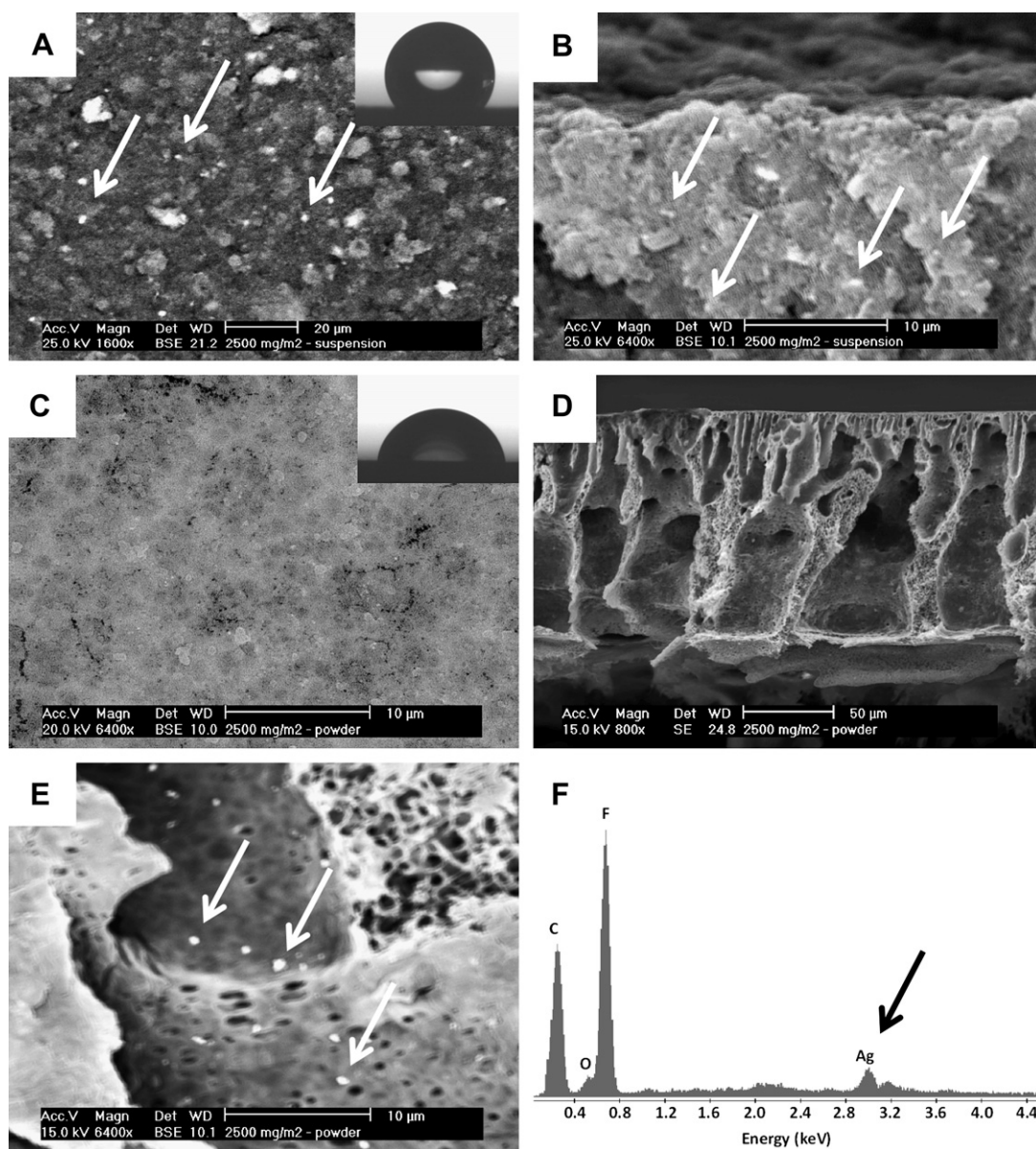


Fig. 1 – SEM images of the PVDF membranes. Figure (A) and (B) present the top surface and the cross section of the membrane containing 2500 mg bio-Ag⁰_{susp} m⁻², respectively. In (C) and (D) the top surface and the cross section of the PVDF membrane containing 2500 mg bio-Ag⁰_{powder} m⁻² are shown, respectively. (E) is a higher magnification picture of the pores of the latter membrane, and (F) represents the EDX spectrum of this detail. The peaks C and F relate to the PVDF matrix. White arrows indicate agglomerates of biogenic silver, visible as enlightened dots in the BSE mode. The inserts in (A) and (C) are the profile of a water droplet on the top surface of the membranes.

membrane was apparent: in the skin layer, pore channels with a small diameter of hundreds of nanometers were present, whereas the sublayer consisted of larger columned pores of several micrometers. In both layers, silver agglomerates were visible as bright dots, as demonstrated by larger magnification (Fig. 1E). The presence of silver throughout this membrane cross section was confirmed by EDX (Fig. 1F). Within these agglomerates, individual particles have been observed, suggesting that the larger silver clusters are in fact the bacterial cell carrier covered with silver nanoparticles.

3.2. Virus inactivation in batch by bio-Ag⁰ immobilized in PVDF membranes

The antiviral properties of the bio-Ag⁰ containing membranes were first examined in batch experiments. Submersion of 25 cm² of the 2500 mg bio-Ag⁰_{susp} m⁻² membrane resulted in a 4.1 log decrease after 24 h of indirect contact with immobilized bio-Ag⁰ (Table 2). To examine the influence of the embedded silver concentration, the same surface area of the 250 mg bio-Ag⁰_{susp} m⁻² membrane was submerged in contaminated water but no virus removal was observed (Table 2). Consistent with these results, analyses of the silver concentrations in the water revealed greater release of Ag⁺ from the 2500 mg bio-Ag⁰_{susp} m⁻² membrane (Table 2). To investigate the influence of the biogenic silver formulation, 25 cm² of the membrane impregnated with 2500 mg bio-Ag⁰_{powder} m⁻² was submerged in the suspension as well. The Ag⁺ release was lower than with the same concentration of bio-Ag⁰_{susp}, yet, the virus inactivation was similar, resulting in at least a 4.3 log decline after 24 h of indirect contact with the immobilized bio-Ag⁰ (Table 2). Moreover, immobilization of 2500 mg m⁻² of both types of bio-Ag⁰ in PVDF membranes seemed to be efficient for more than 3 log virus decrease after only 2 h under the given test conditions.

3.3. Virus inactivation by bio-Ag⁰ immobilized in PVDF membranes in a continuous membrane reactor

Continuous disinfection experiments were conducted in a membrane reactor by filtering contaminated water through a submerged plate, holding the bio-Ag⁰ PVDF membranes. When the 2500 mg bio-Ag⁰_{susp} m⁻² membrane was used in the reactor, no viruses were detected in the effluent after filtration

of 6.3 L m⁻², yielding at least a 3.6 log decrease (Fig. 2A). Interestingly, the virus inactivation in the bulk phase of the membrane unit was the same as in the filtrate (data not shown). Even after filtration of 225 L m⁻², a 2.9 log decline could still be achieved using this membrane. In contrast, the virus removal achieved with the control membrane without bio-Ag⁰ and the membrane containing 250 mg bio-Ag⁰_{susp} m⁻² amounted to no more than 1 log virus removal. Similar results were achieved in the filtration experiments with the membranes containing bio-Ag⁰_{powder} (Fig. 2B). No viruses were detected in the bulk liquid or the filtrate when the 2500 mg bio-Ag⁰_{powder} membrane was used in the reactor, even after filtration of 225 L m⁻². In the case of the 250 mg bio-Ag⁰_{powder} m⁻² however, a maximum virus removal of only 1.2 log was observed. In each reactor run, the transmembrane pressure (TMP) was not higher than 50 mbar. No differences in TMP between the control membrane and the silver containing membranes were observed.

Leaching of Ag⁺ from the 250 mg bio-Ag⁰ m⁻² membranes was very low, with 10.7 µg L⁻¹ being the highest concentration detected in the filtrate (data not shown). Higher concentrations of Ag⁺ were encountered in the effluent of the filtration experiments with the 2500 mg bio-Ag⁰ m⁻² membranes (Fig. 3). At the startup of the membrane reactor, the Ag⁺ concentrations released by the 2500 mg bio-Ag⁰_{susp} m⁻² and the 2500 mg bio-Ag⁰_{powder} membranes reached concentrations up to 236 and 271 µg L⁻¹, respectively. In both cases, the Ag⁺ concentration in the effluent decreased when more water was filtered. Yet, after filtration of 225 L m⁻² through the bio-Ag⁰_{susp} containing membrane, 102 µg Ag⁺ L⁻¹ was still detected in the effluent. The decrease of the Ag⁺ concentration in the effluent was much faster in the case of the bio-Ag⁰_{powder} containing membrane. After filtration of 75 L m⁻² the Ag⁺ release was reduced to 57 µg L⁻¹, whereas no more than 24 µg L⁻¹ was detected in the effluent of the 2500 mg bio-Ag⁰_{powder} membrane after filtration of 225 L m⁻².

Subsequently, another 2500 mg bio-Ag⁰_{powder} m⁻² membrane was applied in the membrane unit and the HRT was decreased from one day to 1 h, resulting in a membrane flux of 75 L m⁻² h⁻¹. At startup of the reactor, no viruses were detected in the filtrate, thus yielding at least a 3.9 log decrease (Fig. 4). After filtration of 112.5 L m⁻² however, low concentrations of phages were detected again in the bulk phase (data not shown)

Table 2 – Virus inactivation and Ag⁺ release by 25 cm² of the different PVDF membranes in a 24 h batch experiment. The concentration of UZ1 is expressed as the mean value of triplicate plaque assays (±standard deviation). The LOD was determined at 1.0 × 10² pfu mL⁻¹.

Membrane	0 h		2 h		24 h	
	UZ1 concentration (pfu mL ⁻¹)	Ag ⁺ release (µg L ⁻¹)	UZ1 concentration (pfu mL ⁻¹)	Ag ⁺ release (µg L ⁻¹)	UZ1 concentration (pfu mL ⁻¹)	Ag ⁺ release (µg L ⁻¹)
250 mg bio-Ag ⁰ _{susp} m ⁻²	6.5 ± 2.7 × 10 ⁶	ND ^a	4.6 ± 0.6 × 10 ⁶	4 ± 2	3.7 ± 0.9 × 10 ⁶	16 ± 4
2500 mg bio-Ag ⁰ _{susp} m ⁻²	3.8 ± 0.8 × 10 ⁶	ND	3.4 ± 5.4 × 10 ³	208 ± 5	3.3 ± 3.2 × 10 ²	792 ± 10
2500 mg bio-Ag ⁰ _{powder} m ⁻²	2.4 ± 0.5 × 10 ⁶	ND	4.9 ± 6.2 × 10 ²	27 ± 8	< LOD	95 ± 6

a ND: not detected (below LOD = 0.8 µg L⁻¹).

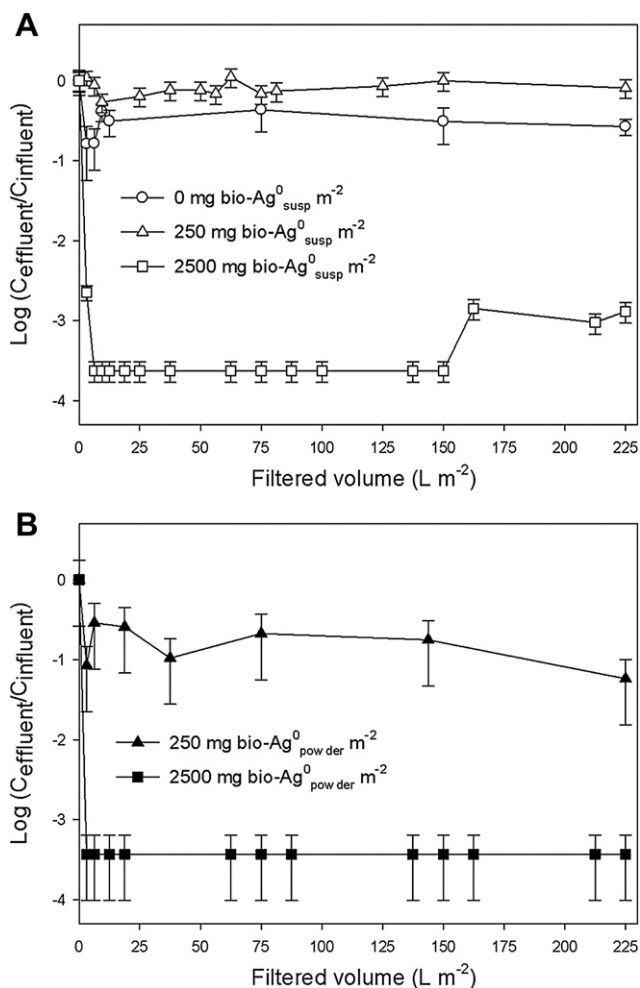


Fig. 2 – Virus inactivation as a function of the filtered volume through (A) PVDF membranes containing 0, 250 and 2500 mg bio-Ag⁰_{susp} m⁻², and (B) 250 and 2500 mg bio-Ag⁰_{powder} m⁻². The HRT of the membrane reactor was 1 day and the maximum detectable virus removal amounted to 3.4 log. C_{influent} = concentration of UZ1 in the influent; C_{effluent} = concentration of UZ1 in the effluent. Error bars represent the standard deviations of triplicate influent and effluent sample measurements.

and in the filtrate (Fig. 4). Yet, a virus decline of more than 3 log was still achieved, even after filtration of 300 L m⁻². The pattern of Ag⁺ release in the filtrate was similar to the experiments at an HRT of one day. At the startup of the reactor, 223 μg Ag⁺ L⁻¹ was detected in the effluent, followed by a decrease towards 95 μg L⁻¹ after filtration of 300 L m⁻². At an HRT of 1 h, the TMP varied between 50 and 100 mbar.

4. Discussion

4.1. Antiviral action of biogenic silver incorporated PVDF membranes

In this study, the applicability of PVDF membranes with impregnated biogenic silver for virus inactivation in water

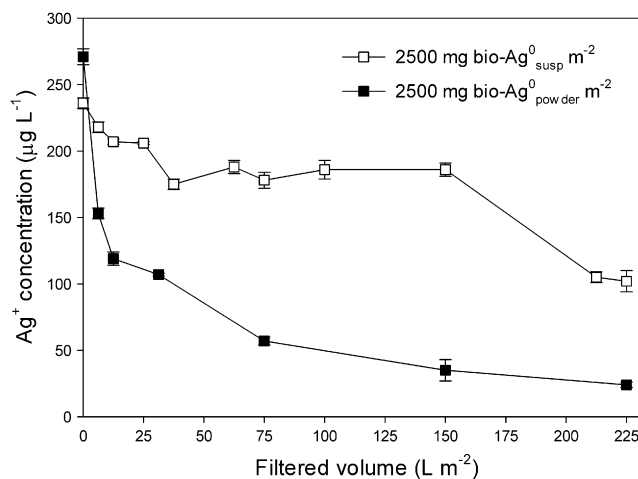


Fig. 3 – Ionic silver released to membrane reactor effluent, as a function of volume filtered through the PVDF membranes containing 2500 mg bio-Ag⁰_{susp} m⁻² and 2500 mg bio-Ag⁰_{powder} m⁻². The HRT of the membrane reactor was 1 day. Error bars represent the standard deviations of triplicate effluent sample measurements.

was demonstrated. Batch experiments showed at least a 4 log decrease of the phages by incorporating 2500 mg bio-Ag⁰ m⁻² in the membranes. Ag⁺ was released from the membranes and its interaction with the UZ1 phages was most probably the main virus inactivation mechanism. Other researchers have demonstrated that AgNO₃ was also effective at inactivating the MS2 and T2 phages and the monkeypox virus (Kim et al., 2008; Richards, 1981; Rogers et al., 2008). Although the antimicrobial action by silver nanoparticles is not fully understood, several studies indicate the importance of Ag⁺ release and the subsequent interaction with thiol groups of bacterial

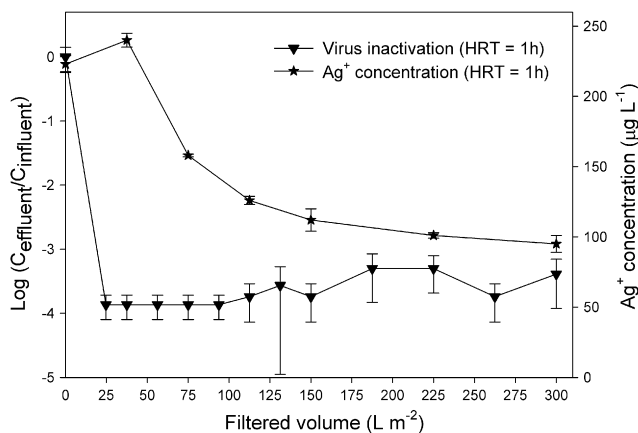


Fig. 4 – Virus inactivation and ionic silver release in the membrane reactor effluent, as a function of the volume filtered through the PVDF membrane containing 2500 mg bio-Ag⁰_{powder} m⁻². The HRT of the membrane reactor was 1 day and the maximum detectable virus removal amounted to 3.9 log. C_{influent} = concentration of UZ1 in the influent; C_{effluent} = concentration of UZ1 in the effluent. Error bars represent the standard deviations of triplicate influent and effluent sample measurements.

enzymes and (glyco)proteins exposed on the bacterial or viral surface, or the reaction with phosphorus containing nucleic acids (Feng et al., 2000; Liau et al., 1997; Matsumura et al., 2003). In addition, the direct interaction of viruses with silver nanoparticles has been suggested to physically obstruct the virus-host cell binding (Elichiguerra et al., 2005; Rogers et al., 2008). However, the latter reaction mechanism seems unlikely to be responsible for the virus inactivation in the present work, since the bio-Ag⁰ particles remained anchored in the polymeric matrix.

4.2. The influence of the embedded concentration and the pre-treatment of biogenic silver on Ag⁺ release by the membranes

From the results of the batch experiments, it was clear that the antiviral properties of the membranes increased with a higher embedded concentration of bio-Ag⁰. Whereas immobilization of 250 mg bio-Ag⁰ m⁻² in the membrane did not result in a significant virus inactivation, the incorporation of 2500 mg bio-Ag⁰ m⁻² clearly enhanced virus disinfection. For both formulations, i.e. bio-Ag⁰_{susp} and bio-Ag⁰_{powder}, similar disinfection efficiencies were obtained at the high concentration. The main difference between the two types was reflected in the Ag⁺ release, with 2500 mg bio-Ag⁰_{susp} m⁻² being the membrane that produced the most ionic silver.

The difference in the two types of pre-treatment resulted in different membrane structures and characteristics as well. Because the oxidation state of the silver nanoparticles themselves remained unaffected after both pre-treatments, the differences tend to be related to the preparation of the casting dopes. Fabrication of the membranes by means of a casting dope with spray-dried bio-Ag⁰ ('bio-Ag⁰_{powder}') did not alter the contact angle and the zeta potential of the membranes, compared to the PVDF membrane without silver. The measured contact angles were in the range of previously reported values for PVDF based surfaces, i.e. 75°–82° (Bormashenko et al., 2006; Peng et al., 2005). Also the negative surface charge of the membranes remained unaffected by the addition of bio-Ag⁰_{powder}, which was also demonstrated by Zodrow et al. (2009). Yet, those authors noticed a decrease in hydrophobicity due to the addition of chemically produced nAg⁰ nanoparticles. The structure of the membranes with bio-Ag⁰_{powder} was typically asymmetric, which can be explained by the fact that no traces of water (the non-solvent) were present in the casting dope. Subsequent immersion in a water bath likely resulted in a fast liquid–liquid demixing prior to polymer precipitation, as described by Cheng et al. (1999). As a result, the membranes showed an asymmetric morphology characterized by a skin layer and a cellular sublayer.

On the contrary, when a wet pellet of biogenic silver particles ('bio-Ag⁰_{susp}') was dispersed in DMF after centrifugation of the bio-Ag⁰ suspension, the resulting casting dope contained a fraction of water (the non-solvent). Submersion of these kinds of dopes increases the crystallization rate of PVDF and a more uniform and dense membrane is formed (Cheng et al., 1999), as observed in the cross section of the bio-Ag⁰_{susp} based membrane. This process can be enhanced by submersion in a non-solvent bath with a fraction of solvent, a so-called 'soft precipitation bath' (Cheng et al., 1999; Peng et al., 2005). The top

surface of these sponge-like membranes is known to exhibit greatly enhanced hydrophobicity and a certain roughness (Peng et al., 2005), which was confirmed by the larger contact angles measured and SEM images in this study.

The addition of bio-Ag⁰_{susp} to the membrane decreased the absolute value of the zeta potential as well. Calculation of the surface charge density according to Hiemenz and Rajagopalan (1997), indicated that the amount of charges per m² on the 2500 mg bio-Ag⁰_{susp} m⁻² was ten times lower than on the 2500 mg bio-Ag⁰_{powder} m⁻² (0.62×10^{-9} vs. 6.46×10^{-9} mol m⁻², respectively). This is likely due to the greater ionic interaction with Ag⁺, initially present in the pellet of bio-Ag⁰_{susp}, and could explain the subsequent greater release of Ag⁺ by the bio-Ag⁰_{susp} membrane. Moreover, the surface of the bio-Ag⁰_{susp} membrane contained more biogenic silver, which likely also facilitated Ag⁺ release. Future research is needed to fully understand how the membrane structure and characteristics can influence the Ag⁺ release from incorporated biogenic silver and the subsequent disinfection of water.

4.3. Application of the membranes for continuous disinfection

The membranes with 2500 mg bio-Ag⁰ m⁻² were successfully used for continuous disinfection of the UZ1 phage in a submerged plate membrane reactor. The fact that similar virus disinfection efficiencies were observed in both the bulk phase and the effluent strongly suggests that direct interaction with the silver particles during passage through the membrane is not the main antiviral mechanism. Ionic silver release was probably the main antiviral mechanism in the continuous disinfection experiments as well. Significant Ag⁺ concentrations were found in the case of the 2500 mg bio-Ag⁰ m⁻² membranes while the Ag⁺ release by the 250 mg bio-Ag⁰ m⁻² membrane and the concomitant virus inactivation efficiencies were low. Again, the Ag⁺ release by the bio-Ag⁰_{susp} membrane was more than what was observed for the bio-Ag⁰_{powder} membrane. The control of the Ag⁺ release by the membrane is important since the drinking water threshold for Ag⁺ is limited to 0.1 mg L⁻¹ by the WHO (2004). From this point of view, the use of bio-Ag⁰_{powder} to fabricate antiviral PVDF membranes seems the best approach since the Ag⁺ release was around or below the threshold value after a certain filtration period (31 L m⁻²).

Also from an economical point of view, a controlled release of Ag⁺ is wanted since rapid depletion of the membrane-associated silver might compromise its long-term performance. Indeed, other researchers have demonstrated that the antimicrobial activity of silver loaded membranes and hollow fibers were greatly decreased due to a decrease of the silver content (Chou et al., 2005; Zodrow et al., 2009). Plate membranes lost their antimicrobial properties after leaching from the membrane surface layer stopped, even though 90% of the added silver particles still remained in the membrane (Zodrow et al., 2009). The application of bio-Ag⁰_{powder} containing membranes might overcome this problem since agglomerates of silver were also encountered at the pore walls inside the membrane, from where they can also contribute to the release of Ag⁺ for virus disinfection. However, since Ag⁺ is slowly released from the membranes, the disinfection effect is expected to decrease over

time. This means that in practice, these membranes can be applied to treat limited volumes of contaminated water (e.g. in refugee camps) but that they cannot be used for continuous long-term and large-scale drinking water production. The membranes must be regarded as a gentle way to provide temporarily low amounts of ionic silver without the risk of releasing nanoparticles, comparable with other slow release techniques for small scale treatment such as polymer-iodine tablets (slowly releasing iodine) or sodium dichloroisocyanurate tablets (slowly producing hypochlorous acid) (Clasen and Edmondson, 2006; Mazumdar et al., 2010).

The results of the batch experiments indicate that the antiviral activity of the bio-Ag⁰ membranes depends on both the released Ag⁺ dose and the contact time, meaning that the HRT is likely an important operational parameter for continuous experiments. Given that > 3 log decline was achieved after only 2 h in batch, an even shorter contact time (1 h HRT) was assessed in the continuous experiments with the 2500 mg bio-Ag⁰_{powder} m⁻² membrane. Even at a flux as high as 75 L m⁻² h⁻¹, high virus inactivation efficiencies were obtained at low TMP values. Yet, viruses were again detected in the effluent after filtration of 112.5 L m⁻², even when the Ag⁺ concentration was as high as 126 µg L⁻¹. This contrasts with the results from the 1 d HRT experiments in which the UZ1 concentration remained below the LOD at Ag⁺ levels lower than 100 µg L⁻¹. More data on the combined effect of Ag⁺ concentration and contact time are needed before one can model adequately the optimal combination between reactor residence time and silver concentration in the membranes.

5. Conclusions

The results of this work show that a bacterial carrier matrix containing silver nanoparticles can be successfully immobilized in microporous membranes where it provides for potent antiviral activity in a submerged plate membrane reactor. Inactivation of UZ1 bacteriophages using these membranes was successfully demonstrated at low and high membrane fluxes, and was most probably related to the slow release of Ag⁺ from the membranes. By increasing our understanding of how the membrane structure affects the release rate of Ag⁺ from bio-Ag⁰, the Ag⁺ concentration in the filtrate could be further decreased and the depletion of Ag⁺ from the material should be controlled. Yet, long-term filtration experiments are required to confirm that this does not compromise the antimicrobial activity. It is expected that due to the gradual release of Ag⁺ from the membranes, their antiviral activity will decrease over time. Therefore, it can be concluded that this technique can be applied for the treatment of limited volumes of contaminated water but not for long-term drinking water production.

Acknowledgements

This work was supported by a PhD grant (B. De Gusseme) and project grant no. 7741-02 (T. Hennebel) of the Research Foundation Flanders (FWO). It was part of project no. G.0808.10N (2010–2013), funded by the FWO. K. Verbeken is

a postdoctoral fellow with the FWO. We gratefully thank Griet Vermeulen, Jan Dick, Pieter Spanoghe and Peter Mast for their technical assistance and Elke De Clerck (Janssen Pharmaceutica NV, Beerse, Belgium) for kindly providing the spray-dried biogenic silver. We acknowledge Anthony Hay, Simon De Corte, Liesje Sintubin and Willem De Muynck for critically reviewing this manuscript and the many helpful suggestions.

Appendix A. Supplementary material

Supplementary data associated with this article can be found, in the online version, at doi:10.1016/j.watres.2010.11.046.

REFERENCES

- Adams, M.H., 1959. Bacteriophages. Interscience, New York.
- Bormashenko, E., Stein, T., Whyman, G., Bormashenko, Y., Pogreb, R., 2006. Wetting properties of the multiscaled nanostructured polymer and metallic superhydrophobic surfaces. *Langmuir* 22 (24), 9982–9985.
- Cheng, L.P., Lin, D.J., Shih, C.H., Dwan, A.H., Gryte, C.C., 1999. PVDF membrane formation by diffusion-induced phase separation-morphology prediction based on phase behavior and mass transfer modeling. *Journal of Polymer Science Part B-Polymer Physics* 37 (16), 2079–2092.
- Chou, W.L., Yu, D.G., Yang, M.C., 2005. The preparation and characterization of silver-loading cellulose acetate hollow fiber membrane for water treatment. *Polymers for Advanced Technologies* 16 (8), 600–607.
- Clasen, T., Edmondson, P., 2006. Sodium dichloroisocyanurate (NaDCC) tablets as an alternative to sodium hypochlorite for the routine treatment of drinking water at the household level. *International Journal of Hygiene and Environmental Health* 209 (2), 173–181.
- De Gusseme, B., Du Laing, G., Hennebel, T., Renard, P., Chidambaram, D., Fitts, J.P., Bruneel, E., Van Driessche, I., Verbeken, K., Boon, N., Verstraete, W., 2010a. Virus removal by biogenic cerium. *Environmental Science & Technology* 44, 6350–6356.
- De Gusseme, B., Sintubin, L., Baert, L., Thibo, E., Hennebel, T., Vermeulen, G., Uyttendaele, M., Verstraete, W., Boon, N., 2010b. Biogenic silver for disinfection of water contaminated with viruses. *Applied and Environmental Microbiology* 76 (4), 1082–1087.
- Elichiguerra, J.L., Burt, J.L., Morones, J.R., Camacho-Bragado, A., Gao, X., Lara, H.H., Yacaman, M.J., 2005. Interaction of silver nanoparticles with HIV-1. *Journal of Nanobiotechnology* 3 (1). doi:10.1186/1477-3155-1183-1186.
- Feng, Q.L., Wu, J., Chen, G.Q., Cui, F.Z., Kim, T.N., Kim, J.O., 2000. A mechanistic study of the antibacterial effect of silver ions on *Escherichia coli* and *Staphylococcus aureus*. *Journal of Biomedical Materials Research* 52 (4), 662–668.
- Hennebel, T., De Gusseme, B., Boon, N., Verstraete, W., 2009a. Biogenic metals in advanced water treatment. *Trends in Biotechnology* 27 (2), 90–98.
- Hennebel, T., Verhagen, P., Simoen, H., De Gusseme, B., Vlaeminck, S.E., Boon, N., Verstraete, W., 2009b. Remediation of trichloroethylene by bio-precipitated and encapsulated palladium nanoparticles in a fixed bed reactor. *Chemosphere* 76 (9), 1221–1225.
- Hennebel, T., De Corte, S., Vanhaecke, L., Vanherck, K., Forrez, I., De Gusseme, B., Verhagen, P., Verbeken, K., Van der Bruggen, B., Vankelecom, I., Boon, N., Verstraete, W., 2010.

- Removal of diatrizoate with catalytically active membranes incorporating microbially produced palladium nanoparticles. *Water Research* 44 (5), 1498–1506.
- Hiemenz, P.C., Rajagopalan, R., 1997. *Principles of Colloid and Surface Chemistry*. Marcel Dekker, New York.
- Kim, J.Y., Lee, C., Cho, M., Yoon, J., 2008. Enhanced inactivation of *E. coli* and MS-2 phage by silver ions combined with UV-A and visible light irradiation. *Water Research* 42 (1–2), 356–362.
- Li, Q.L., Mahendra, S., Lyon, D.Y., Brunet, L., Liga, M.V., Li, D., Alvarez, P.J.J., 2008. Antimicrobial nanomaterials for water disinfection and microbial control: potential applications and implications. *Water Research* 42 (18), 4591–4602.
- Liau, S.Y., Read, D.C., Pugh, W.J., Furr, J.R., Russell, A.D., 1997. Interaction of silver nitrate with readily identifiable groups: relationship to the antibacterial action of silver ions. *Letters in Applied Microbiology* 25 (4), 279–283.
- Mafune, F., Kohno, J., Takeda, Y., Kondow, T., Sawabe, H., 2000. Structure and stability of silver nanoparticles in aqueous solution produced by laser ablation. *Journal of Physical Chemistry B* 104 (35), 8333–8337.
- Matsumura, Y., Yoshikata, K., Kunisaki, S., Tsuchido, T., 2003. Mode of bactericidal action of silver zeolite and its comparison with that of silver nitrate. *Applied and Environmental Microbiology* 69 (7), 4278–4281.
- Mazumdar, N., Chikindas, M.L., Uhrich, K., 2010. Slow release polymer-iodine tablets for disinfection of untreated surface water. *Journal of Applied Polymer Science* 117 (1), 329–334.
- McDonogh, R., Schaule, G., Flemming, H.C., 1994. The permeability of biofouling layers on membranes. *Journal of Membrane Science* 87 (1–2), 199–217.
- Mulder, M., 1991. *Basic Principles of Membrane Technology*. Kluwer Academic Publishers, Dordrecht.
- Peng, M., Li, H.B., Wu, L.J., Zheng, Q., Chen, Y., Gu, W.F., 2005. Porous poly(vinylidene fluoride) membrane with highly hydrophobic surface. *Journal of Applied Polymer Science* 98 (3), 1358–1363.
- Richards, R.M.E., 1981. Antimicrobial action of silver-nitrate. *Microbios* 31 (124), 83–91.
- Rogers, J.V., Parkinson, C.V., Choi, Y.W., Speshock, J.L., Hussain, S.M., 2008. A preliminary assessment of silver nanoparticle inhibition of monkeypox virus plaque formation. *Nanoscale Research Letters* 3 (4), 129–133.
- Rose, J.B., Gerba, C.P., 1991. Assessing potential health risks from viruses and parasites in reclaimed water in Arizona and Florida, USA. *Water Science and Technology* 23 (10–12), 2091–2098.
- Saveyn, H., Pauwels, G., Timmerman, R., Van der Meeren, P., 2005. Effect of polyelectrolyte conditioning on the enhanced dewatering of activated sludge by application of an electric field during the expression phase. *Water Research* 39 (13), 3012–3020.
- Sintubin, L., De Windt, W., Dick, J., Mast, J., van der Ha, D., Verstraete, W., Boon, N., 2009. Lactic acid bacteria as reducing and capping agent for the fast and efficient production of silver nanoparticles. *Applied Microbiology and Biotechnology* 84 (4), 741–749.
- Tilton, R.C., Rosenberg, B., 1978. Reversal of silver inhibition of microorganisms by agar. *Applied and Environmental Microbiology* 35 (6), 1116–1120.
- Ueda, T., Horan, N.J., 2000. Fate of indigenous bacteriophage in a membrane bioreactor. *Water Research* 34 (7), 2151–2159.
- USEPA, 2009. Drinking water contaminant candidate list 3-final. *Federal Register* 74 (194), 51850–51862.
- Vankelecom, I.F.J., 2002. Polymeric membranes in catalytic reactors. *Chemical Reviews* 102, 3779–3810.
- Verthé, K., Possemiers, S., Boon, N., Vanechoutte, M., Verstraete, W., 2004. Stability and activity of an *Enterobacter aerogenes*-specific bacteriophage under simulated gastrointestinal conditions. *Applied Microbiology and Biotechnology* 65 (4), 465–472.
- WHO, 2004. *Guidelines for Drinking Water Quality*. World Health Organization, Geneva, Switzerland.
- Wu, J.L., Li, H.T., Huang, X., 2010. Indigenous somatic coliphage removal from a real municipal wastewater by a submerged membrane bioreactor. *Water Research* 44 (6), 1853–1862.
- Yang, H.L., Lin, J.C.T., Huang, C., 2009. Application of nanosilver surface modification to RO membrane and spacer for mitigating biofouling in seawater desalination. *Water Research* 43 (15), 3777–3786.
- Zodrow, K., Brunet, L., Mahendra, S., Li, D., Zhang, A., Li, Q.L., Alvarez, P.J.J., 2009. Polysulfone ultrafiltration membranes impregnated with silver nanoparticles show improved biofouling resistance and virus removal. *Water Research* 43 (3), 715–723.